Analyst

Accepted Manuscript

ROYAL SOCIETY OF CHEMISTRY

www.rsc.org/analyst

Analyst

RSCPublishing

ARTICLE

Carboxy-Terminated Immuno-SERS Tags Overcome Non-Specific Aggregation for the Robust Detection and Localization of Organic Media in Artworks

Cite this: DOI: 10.1039/x0xx00000x

Received 00th March 2015,
Accepted 00th January 2012

DOI: 10.1039/x0xx00000x

www.rsc.org/

E. A. Perets[a], A. S. D. S. Indrasekara[b], A. Kurmis[a], N. Atlasevich[a], L. Fabris[b], and J. Arslanoglu[a]

Methods combining immunology and surface-enhanced Raman scattering (SERS) have been developed for the simultaneous detection, identification, and localization of proteinaceous binding media found in artworks. However, complex surface topographies and heterogeneous compositions of art samples represent significant challenges for the general optimization of this technique. In particular, aggregation of immuno-SERS nanoparticles can lead to non-specific SERS response across the sample surface, resulting in inaccurate identification of binding media or dubious localization maps. This aggregation also diminishes the sample area available for analysis, as excitation of visible nanoparticle aggregates by the Raman laser must be avoided during data collection. In the present work, we synthesize several types of immuno-SERS nanoparticles and investigate their applicability for the detection and localization of ovalbumin-rich (egg-based) binding media in art samples. Dimers of gold nanoparticles (Au NPs) connected by a Raman-active dithiolated linker are conjugated to secondary antibodies through either an amino or carboxyl functional group (SERS tags). The SERS tags display localized surface plasmon resonance (LSPR) at 532 nm. SERS spectra are acquired at 633 nm (SERS-633) in order to maximize tuning between laser excitation and LSPR, while avoiding sample burning. In an indirect immunoassay applied to replica art samples, carboxy-terminated SERS-633 tags show strong Raman reporter signal, specificity for the target protein, robust response in the presence of various inorganic pigments, and reduced aggregation on sample surfaces compared to amino-terminated or commercial SERS tags. Scanning electron microscopy (SEM) is used to visualize Au NPs bound to egg media *in situ*, demonstrating that carboxy-terminated SERS-633 tags remain as discrete dimer units throughout the assay.

Formatted: Spanish (International Sort), Expanded by 0.2 pt

Formatted: Spanish (International Sort)

Comment [EP1]: Referee: 2

Introduction

Accurately understanding the composition of artworks is critical for the art historical record and the preservation of heritage objects. Recently, several antibody-based techniques have been adapted for the detection of proteins and gums in artworks. Though previously established methods such as the enzyme-linked immunosorbent assay (ELISA) [1] and dot-blot analyses [2] are extremely sensitive and selective, these techniques preclude localization data of proteinaceous materials within the stratigraphy of a polychrome cross-section because they require extraction of the organic material into solution. Techniques that preserve this information, including attenuated total reflectance Fourier transform infrared spectroscopy (ATR-FTIR) and secondary ion mass spectrometry (SIMS), can demonstrate the presence of proteinaceous media but are often highly ambiguous with regard to protein identity [3-5]. Immunological detection methods with fluorescent reporting systems struggle against the high, naturally occurring fluorescence found in paint cross-sections [6]. The more successful reporting systems using quantum dots [7] and chemiluminescence [8] require instrumentation not readily available to cultural heritage scientists. The application of surface enhanced Raman scattering (SERS)-based reporting systems for the immunological detection of proteins offers several advantages over other protein imaging techniques, including the amplification of an identifiable reporter signal above background autofluorescence within the sample

environment. In addition, Raman microscopy is a common technology in the field of cultural heritage for its ability to molecularly identify inorganic and organic colorants with a variety of lasers, and its widespread availability. Another potential major advantage for in-field cultural heritage applications includes the recent development of portable Raman spectrophotometers, relatively inexpensive handheld devices with high-performance SERS-sensing capabilities [9].

Controlled fabrication of nanostructured sensing platforms, or tags derived from precious metals such as silver and gold, has facilitated the development of technologies for the detection of various inorganic and biological substrates [10]. Many such technologies have harnessed resonance effects from interactions between the metal and unlabelled or fluorescently-labelled targets. These include Förster resonance energy transfer (FRET) systems [11], and surface plasmon resonance (SPR) variations due to adsorption of single molecules [12]. SERS approaches have received attention because of the heightened sensitivity to Raman-active small molecules when located close to a metal surface [13]. If the molecule is located at the interstitial gap, or "hot spot", between assembled nanoparticles, then increases in SERS signal intensities up to ten orders of magnitude may be observed [14]. Recently, SERS enhancement factors on the order of ~10^{11} have been experimentally demonstrated for *bottom-up* assemblies of gold dimer-on-mirror nanostructures and nanostars [15, 16]. These signal enhancements can be exploited in sensing applications by rationally designing SERS tags with high signal intensity and high selectivity toward specific target molecules. A SERS tag is generally constituted of four components: (i) one or more plasmonic nanoparticles that contribute to electromagnetic and chemical enhancements; (ii) a Raman reporter whose SERS signal can be followed to locate the target; (iii) a stabilizing silica or polyethylene glycol (PEG) layer to impart stability to the tag; and (iv) one or more targeting molecules (e.g., antibodies) that specifically recognize and bind the analyte of interest. SERS tags have enabled the highly sensitive, specific detection of antigenic materials via direct and indirect immunoassay methods, and are therefore promising tools for the identification of proteinaceous materials in artworks [17-20].

Recently, immunological-SERS methods have been suggested as a simple alternative for both the detection and localization of organic materials in artworks [21, 22]. The

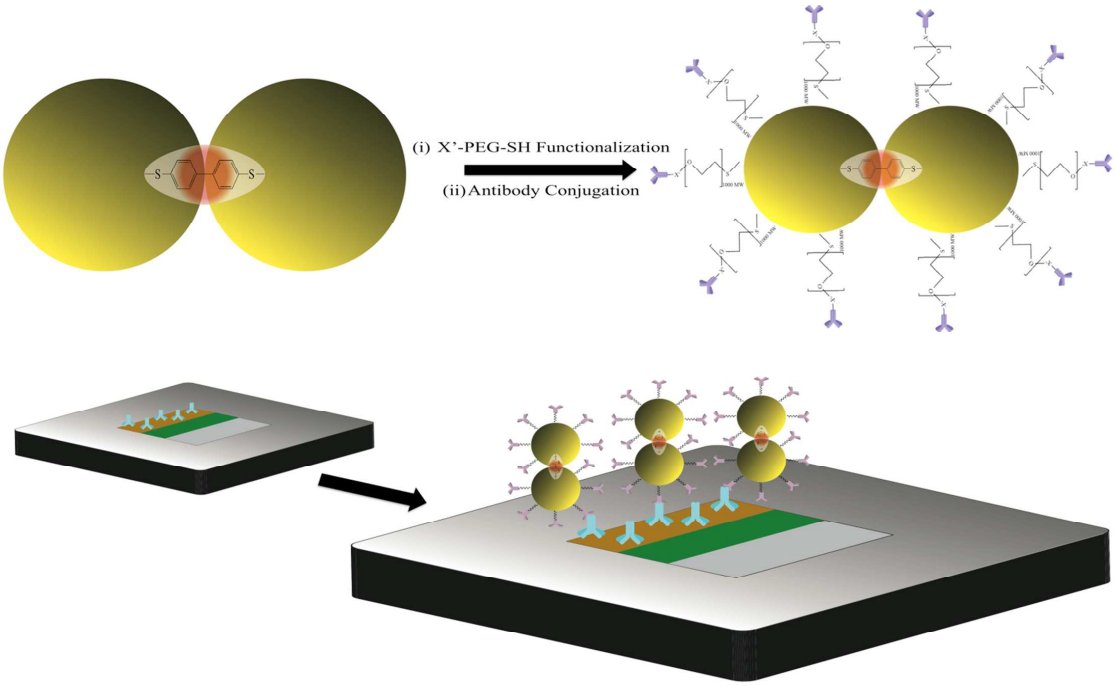

Figure 1. Schematic of SERS-633 Au NP functionalization and immuno-SERS assay. Au NPs (golden spheres) are dimerized via Raman-active biphenyl-4, 4'-dithiol (DBDT) reporter at the "hot spot" (red sphere) and surface functionalized with X'-PEG-SH coating (MW 1000, X' = -NH_2 or -COOH). Conjugation to polyclonal secondary antibody (purple) is achieved through DCC/NHS conjugation chemistry. First, a mounted cross-sectional sample (bottom) is incubated with polyclonal primary antibody (light blue). Next, excess primary antibody is removed with washing, and SERS-633-tagged secondary antibodies are applied. Au NPs are localized only to those regions of the sample where antigen is present.

Comment [EP4]: Referee: 3, Comment (2)

Comment [EP2]: Referee: 3, Comment (3)

Comment [EP3]: Referee: 3, Comment (1)

experimental scheme presented here utilizes the controlled synthesis and dimerization of surface-functionalized gold nanoparticles as reporting systems for protein-rich binding media in cross-sectional art samples (**Figure 1**).

In general, an art sample may be composed of multiple, distinct paint layers, or else a more complex mixture of several pigments and organic binders. Each paint layer consists of a pigmented or unpigmented matrix bound in an organic medium, in this case a proteinaceous binding medium. The total amount of protein-binder can be roughly estimated as 10% of the total mass of the paint. A three-dimensional art sample is mounted in resin, and dry-polished to achieve the smoothest surface possible. In contrast to simple monolayer preparations, exposed sample surfaces will be heterogeneous. Due to the inhomogeneity of mixing during paint preparation, the amount of protein exposed on the surface of the polished cross-section may be significantly lower than the bulk protein presence. The protein-binder is held in a rigid matrix through interactions with pigment particles, and the chemistry of drying and ageing [23].

In the indirect immuno-SERS scheme, primary antibodies are applied at the surface of the sample. The target protein (antigen) on the sample surface is detected through binding of the primary antibody by SERS-633 tagged secondary antibodies, which are covalently linked to the gold nanoparticles. After Raman analysis, the cross-sections are dried, and the antibodies and tags can be polished away from the sample surface. Cross-sections can then be reused for additional experiments. The presence of small pits and crevices due to the composition of the sample will be ubiquitous across the sample surface regardless of the level of polish. Even if the antigen is present and epitopes exposed on the sample surface, heterogeneity of surface structure can adversely affect epitope recognition by antibodies. The ability to probe only those epitopes that are present at the surface of the cross-section further reduces the chances of detection by antibodies, dramatically increasing the complexity of the analysis. Polyclonal antibodies are used here to overcome this unknown and highly variable factor by probing as many epitopes as possible.

The immuno-SERS protocol must also overcome aggregation of Au NPs if it is to be developed as a reliable technique for the detection and localization of proteins in artworks. The appearance of Au NP aggregates may result from non-specific interactions between secondary antibodies and the sample, physical clumping in the interstices of the sample surface, or tendencies toward self-aggregation as a result of electrostatic interactions. Furthermore, previous reports have observed commercially-available SERS tags to be prone to non-specific aggregation in the analysis of multilayer cross-sectional art samples [21, 22]. These observations directed our interest towards the development of SERS tags specifically optimized for protein detection in a mineral matrix, and thus for the analysis of artworks. Herein, two hetero-bifunctional surface coatings of the form X'-PEG-SH (MW 1000, X' = -NH_2 or -COOH) are synthesized and explored for their abilities to prevent non-specific aggregation of SERS-633 tags. Amino-terminated and carboxy-terminated thiolated PEG allow for simple conjugation to secondary antibodies after covalent attachment to Au NPs. Replica samples prepared and aged in the laboratory were probed for the selective detection of protein binders in the presence of various pigments.

Experimental

Synthesis and Characterization of Functionalized Au NPs

The synthesis of citrate capped spherical Au NPs, and the preparation of Au NP dimers (SERS-633) were carried out as previously reported [24]. Amino-terminated and carboxy-terminated dimers were obtained by quenching the dimerization reaction with hetero-bifunctional PEG (NH_2-PEG-SH MW 1000 Nanocs Inc., and COOH-PEG-SH MW 1000 Nanocs Inc., respectively).

UV-Vis spectra were recorded on a Nanodrop 3000 spectrometer (Thermo Scientific). The morphology of Au NPs was evaluated using a Topcon 002B transmission electron microscope. Au NP suspensions were prepared for Raman analysis by drop casting the sample on a silicon wafer; SERS spectra were acquired using a Renishaw in Via Raman microscope. The spectra were obtained with 633 nm HeNe laser excitation (data acquisition time 1 s, single accumulation, laser power 25 mW) under 20x objective.

Conjugation of Functionalized SERS Nanoparticles to Secondary Antibody

Both amino-terminated and carboxy-terminated Au NPs were conjugated to polyclonal secondary antibody according to the following protocol [24]: 1 mM solutions of N,N'-dicyclohexylcarbodiimide (DCC) (ACROS Organics; 538-75-0) and N-hydroxysuccinimide (NHS) (ACROS Organics; 6066-82-6) were prepared in dimethylformamide. 50 µL each of DCC and NHS solutions were combined and diluted in 2 mL of 3 nM SERS-633 followed by the immediate addition of 200 µg of secondary antibody (Jackson ImmunoResearch; AffiniPure Goat Anti-Rabbit (H+L); 111-005-003). After 24 hours at 4 °C, bovine serum albumin (BSA) (Fisher-Scientific; S-15898) in 1X PBS (Fisher-Scientific; M-5402) was added to a final concentration of 1 µM in order to prevent the adhesion of antibody-nanoparticle conjugates to Eppendorf tubes during purification. Antibody-nanoparticle conjugates were centrifuged for 20 minutes at 1681 g, and the pellet was re-suspended in 20 mM phosphate buffer (0.2:1 volumetric ratio of 0.2 M monophosphate:diphosphate (ACROS Organics; 7558-80-7 and 7782-85-6, respectively), diluted 1:10 in deionized water; pH = 7.5) containing 0.1% BSA (w/v) and 0.05% sodium azide (w/v) (Sigma Aldrich; S2002). Centrifugation and re-suspension of antibody-nanoparticle conjugates was repeated four times. Purified SERS-633 tags were stored at 4 °C until further use.

UV-Vis spectra were collected between 180 and 700 nm (0.5 nm resolution) using an Agilent Cary 50 UV-Vis spectrophotometer. Data were collected in order to verify the successful conjugation of SERS-633 to the secondary antibody

Comment [EP5]: Referee: 2

Comment [EP6]: Referee: 2: Figure 2d was collected between 400 nm and 700 nm, and shows the plasmon resonance arising from the gold colloids (note that the plasmon resonance at 633 nm is always buried beneath this peak). The UV-Vis range of 180-600nm reported here refers to monitoring the conjugation of antibody to the SERS-633 nanoparticles (Figure 2e, in particular); the peak of interest (showing presence of conjugated antibody) is in the region between 250 nm and 290 nm. I have changed the numbers to reflect the wider range shown in Figure 2d. Also, readers may refer to [21] for further SERS-633 characterization data.

by observing changes in the optical spectra. The resuspension buffer contains 1% BSA and registers a narrow peak centred at 290 nm. In the presence of SERS-633, increased absorbance between 250 nm and 290 nm (from secondary antibody) as well as a broad peak centred at 523 nm supports successful conjugation.

Commercial SERS-440 tags (Oxonica) were conjugated to secondary antibody as previously reported [21]. Trans-1,2-bis(4-pyridyl)-ethylene is the Raman-active reporter molecule. Conjugation was monitored by UV-Vis spectrophotometry for increased absorbance between 250 nm and 290 nm.

Replica Sample Preparation and Mounting

Replica Sample 1: Layers of whole egg-bound French ochre paint (Kremer; #40050), casein-bound green earth paint (Kremer; #41800), and animal glue-bound gesso ground (Kremer; Bologna #58100 and Champagne #58000) were applied on a wooden panel. This sample board was approximately 8 years old at the time of analysis.

Replica Sample 2: Whole egg-bound vermilion pigment was added on a gesso ground affixed to glass slides. This sample was approximately 1.5 years old at the time of analysis.

Cross-sectional samples measuring between 1 and 1.5 mm in length were mounted in Technovit 2000 LC resin. Samples were polished to a smooth finish with a MOLART XS-hand polisher (JAAP Enterprise for MOLART Advice) and MicroMesh polishing cloths ranging from 1,500 to 12,000 mesh.

Immuno-SERS Protocol and Measurement

Cross-sectional samples were analysed according to the following protocol. First, mounted samples were treated with mild shaking in 25 mL blocking buffer of Silk® Original soy milk (0.03 grams protein/mL) and 2.5% BSA (w/v) for 1 hour at room temperature. Next, the samples were washed four times with mild shaking for 2.5 minutes in 10 mL of 0.1 M Tris base (adjusted to pH = 7.5 using 30% HCl) containing 1% BSA (w/v), for a total wash time of 10 minutes. 25 µL of rabbit anti-ovalbumin (Sigma-Aldrich) polyclonal primary antibody (diluted 1:1000 in 5% newborn calf serum (v/v) in 1X PBS) were applied to the surface of the cross-sections, and kept overnight at 4 °C. Samples were then washed four times with mild shaking in 10 mL of 1X PBS, giving a total wash time of 10 minutes. The resin around the cross-section was hand-dried, while being careful not to disturb the sample surface previously exposed to primary antibody. Next, 25 µL of SERS-633 conjugated tags (diluted 1:5 in 5% NCS (v/v) in 1X PBS) or SERS-440 conjugated tags (diluted 1:75 in 5% NCS (v/v) in 1X PBS) were applied to the surface of the cross-sections, and incubated for 30 minutes at 37 °C. Samples were washed with 1X PBS for 10 minutes with mild shaking. Samples were then dried at room temperature until ready for measurement.

All immuno-SERS measurements were recorded between 397 and 1788 cm^{-1} (resolution of 3 to 5 cm^{-1}) using a custom-built SENTERRA Raman spectroscope (detector model: DV420A-OE-152) assembled by Bruker Optics and configured with an Olympus BX51 optical module. Replica Sample 1 cross-sections exposed to SERS-633 and commercial SERS-440 tags were probed under 20x objective with excitation wavelength of 633 nm and 5 mW HeNe laser for 20 seconds (except where autofluorescence arising from the gesso ground saturated the detector, in which case the integration time was 10 s). Replica Sample 2 cross-sections exposed to commercial SERS-440 tags were analysed under 20x objective with laser excitation of 785 nm at 10 mW power for 10 seconds; SERS-633 tags were probed with excitation of 633 nm at 2.5 mW for same duration. Power and integration times were lower compared to Replica Sample 1 since the vermilion (mercury sulfide) pigment burned at higher laser power, or saturated the detector at lengthier integration times. At least five spectra were collected from positions selected at random within the paint layers, and analysed using OPUS 7.0 software. Ambient background contributions were subtracted from all SERS spectra. The average counts of spectra collected from spots within a single paint layer are reported herein. Small oscillations in the spectra at λ_0 = 633 nm are thought to be the result of etaloning, i.e. laser excitation interferences originating at multiple surfaces within the stratigraphy of the samples. Such interferences are more evident with laser excitations in the near IR—IR region (J. Lombardy, CUNY, and S. Zaleski, Northwestern University, personal communication).

Comment [EP8]: Referee: 2

Comment [EP7]: Referee: 2: We have removed the name, which is included in the acknowledgments.

Comment [LF9]: Referee: 2: We have calculated the etalon thickness to be ~35 µm.

Raman Data Analysis

Averaged Raman spectra were corrected using the concave rubber band algorithm (100 iterations), then smoothed over 25 points within the Opus 7.0 software platform. Due to the presence of multiple oscillatory peaks from incoming laser interferences at the sample surface (see above), all spectra were exported to OriginPro v8.6 (OriginLab, Northampton, MA) and automatically fit for a single peak using the amplitudinal Gaussian peak function (GaussAmp), which follows the distribution:

$$y = y_0 + Ae^{-(x-x_c)^2/2w^2} \quad (1)$$

where y_0 is the offset, x_c is the centre, w is the width, and A is the amplitude of the curve [25]. Because the most prevalent signal arises from the SERS-633 reporter as a single peak at 1585 cm^{-1}, the presence (or absence) of a defined Gaussian distribution centred about this wavenumber was interpreted as a positive (or negative) result when analysing the spectra. Use of a Gaussian distribution for fitting the collected spectra was justified on the basis of probing a solid cross-section for the presence of SERS tags, where the coherence lifetime (τ_c) is expected to be much greater than the amplitude correlation time (τ_a) of the tags [26].

Visible Light and Scanning Electron Microscopy

Visible light images were collected using a Zeiss Axio Imager.Z2m optical light microscope. Z-stack frames were

captured at 1.470 µm steps under 20x magnification and polarized light, and processed using Axiovision 4.8.1 software.

Scanning electron micrographs were collected with a FE-SEM Zeiss Σigma HD equipped with an Oxford Instrument X-Max^N 80 SDD detector. Samples were coated with a 10 nm carbon layer before imaging. Backscattered detector (BSD) images were collected at a working distance of 5 mm and 5 kV. Mixed SE-BSD images were collected at 10kV and 60% backscatter.

Results and Discussion

SERS tags (SERS-633) were prepared by controlled dimerization of spherical Au NPs (25±2 nm) using biphenyl-4, 4'-dithiol (DBDT) as the Raman-active linker molecule [24].

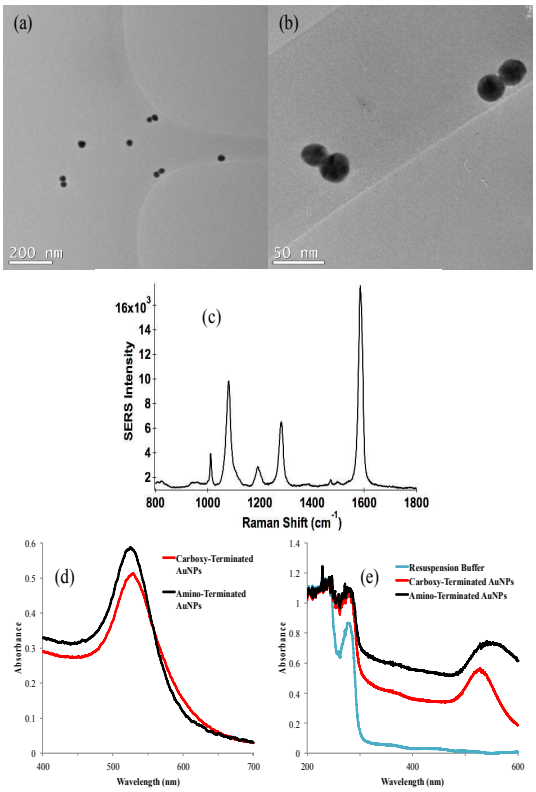

Figure 2. Characterization of X'-PEG-SH functionalized and secondary antibody conjugated AuNP dimers. TEM imaging (a-b), reference SERS spectrum of DBDT reporter signal (c), UV-Vis absorption spectra of PEG functionalized (d) and antibody-conjugated (e) SERS-633.

The dimerization reaction was quenched via addition of thiolated PEG, which also provides colloidal stability. In the present study, we used two sets of SERS-633 tags that are capped with amino- and carboxy-terminated PEGs. Several characterization methods ensured successful assembly of the SERS-active particles (**Figure 2**). TEM micrographs reveal that the morphology of both amino-terminated and carboxy-terminated Au NP dimers (SERS-633) are 50 nm in total length with an average internanoparticle gap of 1-2 nm (**Figure 2a, 2b**). The SERS signal of the reporter molecule, DBDT, was fully detectable and exhibited the expected peak pattern and SERS enhancement (**Figure 2c**). Typical enhancement factors for the dimer-based tags have been evaluated [24], giving rise to values that are at least 1000 times higher than those of their monomeric counterparts. UV-Vis spectra of amino-terminated and carboxy-terminated SERS-633 tags show peaks centered around 523 nm arising from the plasmon resonance of gold colloids (**Figure 2d**). Carboxy-terminated SERS-633 tags showed a slight red shift and damping compared to amino-terminated SERS-633 tags, in agreement with previous reports [27-29]. These effects are indicative of successful coordination of the functionalized coatings in both cases. Additionally, UV-Vis spectra were collected after conjugation of polyclonal secondary antibody to functionalized SERS-633 (**Figure 2e**). The spectra showed increased absorbance at 280 nm, thus supporting higher protein concentrations in the SERS tag suspensions after purification, and successful conjugation.

Comment [LF10]: Referee: 3, Comment (4)

As noted above, the concentration of antigen with epitopes exposed at the surface of any art sample cannot be known precisely. A routine blocking procedure not optimized to unique sample conditions may therefore prove insufficient to prevent non-specific binding and aggregation of Au NPs across the sample surface [21, 22]. It is therefore advisable that other analytical techniques such as FTIR, ATR-FTIR, gas chromatography-mass spectrometry (GCMS) or high-performance liquid chromatography (HPLC) be used to characterize the organic binders present, as a complement to the immuno-SERS analysis. Moreover, the indirect immuno-SERS assays must be optimized (with reference to a control sample) for both primary and secondary antibody-tagged Au NP concentrations after each new antibody-Au NP conjugation.

In this work, Replica Sample 1 consisted of three pigment/binder combinations in discrete layers, including: (i) French ochre/whole egg-bound (~60 µm wide), (ii) green earth/casein-bound (~60 µm wide), and (iii) natural chalk/animal glue-bound cross-sectional layers. The design of this sample allowed us to explore polyclonal primary antibody specificities for common proteinaceous binding media in the presence of different inorganic mineral pigments (**Figure 3**).

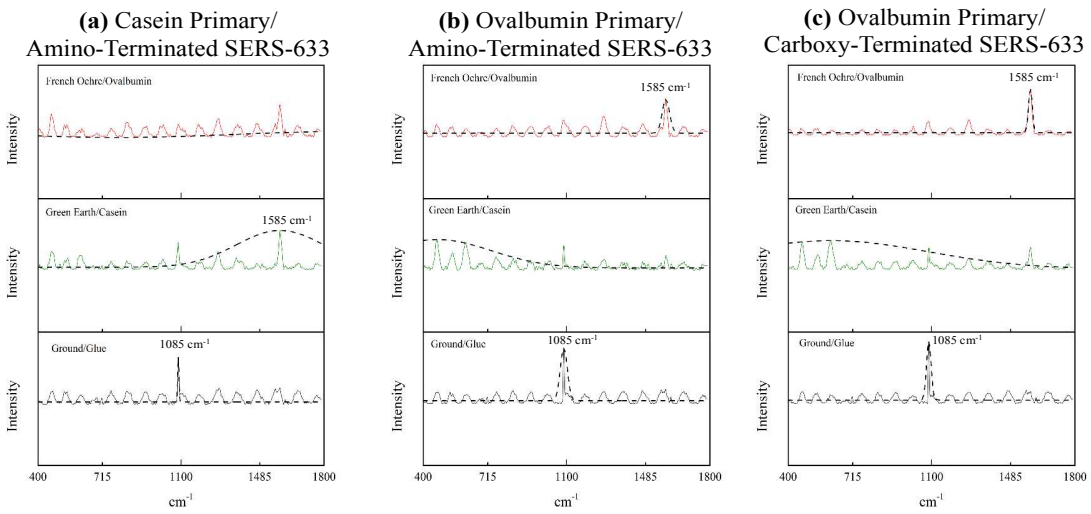

Figure 3. Averaged immuno-SERS spectra from Replica Sample 1 demonstrate primary antibody specificity of amino-terminated and carboxy-terminated SERS-633 tags. Application of (a) anti-casein primary and amino-terminated SERS-633 to Replica Sample 1 shows strong signal only in the green earth/casein layer at 1585 cm^{-1} (characteristic of the SERS reporter). Application of anti-ovalbumin primary and (b) amino-terminated SERS-633 or (c) carboxy-terminated SERS-633 AuNPs shows strong signal only in the French ochre/ovalbumin layer. Experiments also show a strong, sharp peak at 1085 cm^{-1} in the ground/glue layer corresponding to the symmetric CO_3^{2-} stretch, indicative of the presence of calcite ($CaCO_3$). All spectra were collected with a 20x objective and 633 nm He Ne laser excitation (20 s integration time, 5 mW). Spectra are baseline corrected and automatically fit to a single amplitude Gaussian (dashed line).

When polyclonal anti-casein primary and amino-terminated SERS-633 tags were applied to a cross-section prepared from Replica Sample 1, significant reporter signal from DBDT was observed only in the green earth/casein-bound layer, showing that SERS-633 tags were localized to this layer (**Figure 3a**). Therefore, the target protein casein was also localized in that particular layer. When the polyclonal anti-ovalbumin primary antibody was applied with either amino-terminated (**Figure 3b**) or carboxy-terminated (**Figure 3c**) SERS-633 tags, significant reporter signal was observed only in the French ochre/whole egg-bound layer. These results support that localization of SERS-633 tags is dependent upon the specificity of the primary antibody used, and is not influenced by differences in Au NP surface functionalization. Thus, our indirect immuno-SERS protocol accurately captures spatial distributions of protein media in cross-sections prepared from art samples as a result of primary antibody binding to the antigen.

It should be noted that peaks besides those at the characteristic 1585 cm^{-1} are not due to the SERS-633 tags, but can be attributed to natural Raman perturbations of mineral pigments within the system. For example, the spectral peak pattern observed between 400 and 715 cm^{-1} is typical of the presence of glauconite found in many commercial green earth pigments [30]. A single, sharp peak at 1085 cm^{-1} in the preparation layer is attributed to the symmetric CO_3^{2-} stretching mode associated with the presence of a calcite (calcium carbonate, $CaCO_3$) ground preparation layer [31, 32].

The surface matrix of an art sample is both physically variegated and chemically complex, and thus incommensurate with homogenous monolayer preparations common to other SERS-based systems. Therefore, spectroscopic analyses will depend upon the chemical composition of samples, as well as the structure of materials at the sample surface. In particular, the sample area analysed will be affected by both the presence and organization of materials that scatter light. The appearance of calcite peaks in spectra from the green earth/casein-bound layer of Replica Sample 1 suggests that light scatter of the Raman laser beam at λ_0 = 633 nm is of a larger diameter than that predicted for the diffraction limited spot size (~2 µm under 20x objective, calculated as 1.22 λ_0/numerical aperture). Because of this, three observations concerning the application of SERS-based indirect immunoassays to art samples should be acknowledged.

First, because proteins are heterogeneously distributed over the sample surface, background spectra cannot be subtracted on the basis of protein autofluorescence at spots selected randomly within the sample. Furthermore, if SERS tags are present within an area of analysis, background fluorescence of pigment and binding media cannot be systematically separated from the measured SERS spectrum. Thus, the appearance of significant reporter signal above background protein and pigment autofluorescence must be interpreted as a non-quantitative representation of the actual SERS effect induced in reporter-antibody complexes present on the sample.

Second, although collection efficiency generally increases with higher numerical aperture of the Raman microscope objective, it is important that variability inherent to the sample system be investigated for optimal data collection. Aspects of

Comment [EP11]: Referee: 2

Comment [LF12]: Referee: 2

the sample to be controlled include sensitivity of materials to burning at higher magnifications and laser powers, as well as layer thicknesses within the stratigraphy of the cross-section. In some cases, laser coverage of the paint layer may be more critical for signal acquisition than the production of higher energy vibrational perturbations. Assays of Replica Sample 1 at λ_0 = 633 nm under 50x objective (diffraction limited spot size ~1.5 µm) demonstrated similar signal peak intensities and specificity of SERS-633 tags for the antigen of interest as observed under 20x objective (**Figure S1**).

Third, for experiments involving the application of anti-ovalbumin primary antibody, the appearance of any minor peaks at 1585 cm^{-1} in spectra collected from the green earth/casein-bound layer suggest that light scattering from the laser beam (which should be expected due to the high surface roughness of the samples) may have the potential to generate SERS signal from tags located outside the area of the beam spot. However, any SERS signal observed in the green earth/casein-bound layer is of far less intensity than that from natural Raman scattering in the same layer. This becomes readily apparent when a single Gaussian peak is automatically fit to the spectra (**Figure 3**, dashed lines; see Experimental). This data treatment provides a straightforward, efficient, and unambiguous method for the identification of SERS tag signal peaks in spectra with high background signal, which may arise from either sample autofluorescence, or interference due to multiple reflections of excitation laser light at the sample surface [33]. After this data treatment, only the band centred at 1585 cm^{-1} should be treated as significant indicator of SERS-633 secondary antibody localization within the stratigraphy of the cross-section. Analysis of the impact of sample autofluorescence on the sensitivity of the identification method deserves further attention. Additional experiments are currently underway in our laboratories.

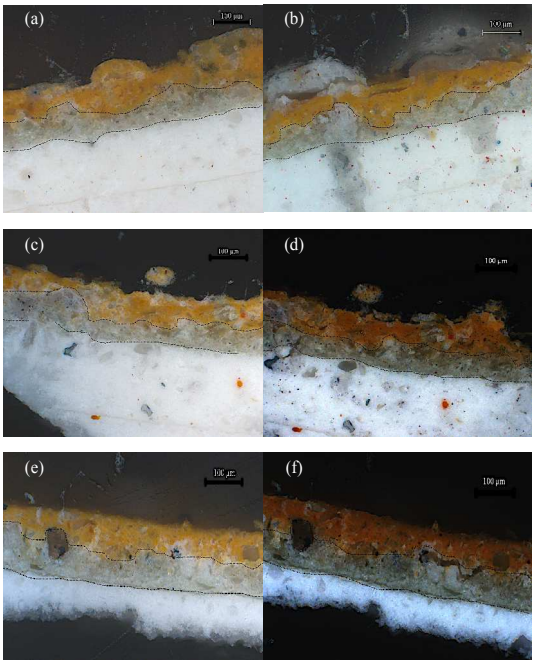

Figure 4. Cross-sectional images of Replica Sample 1 before (left) and after (right) incubation with (a-b) commercial SERS-440, (c-d) amino-terminated SERS-633, and (e-f) carboxy-terminated SERS-633. Commercial SERS-440 and SERS-633 aggregates appear on the sample surface as small crimson or black dots, respectively. Carboxy-terminated SERS-633 show reduced non-specific aggregation. All images collected with polarized light at 20x magnification using Z-stack acquisition. Boundaries between layers (from top: French ochre/ovalbumin, green earth/casein, ground/glue) are given as dashed lines.

Visual analysis of the samples is crucial to optimization and evaluation of the immuno-SERS assay due to the possibility of self-aggregation of Au NPs across the sample surface. Indeed, the widespread presence of large Au NP aggregates has been noted as a major obstacle to the development of reliable and robust SERS-based indirect immunoassays [22]. The formation of Au NP aggregates may remain unavoidable even after proper blocking of the sample and optimization of the assay. Commercial SERS-440 Au NPs were previously investigated for application to art samples [21], and also formed aggregates across the sample surface and resin mount (**Figure 4b**). Likewise, amino-terminated SERS-633 tags appeared as black dots distributed widely across the sample surface even after thorough washing (**Figure 4d**). Significantly, scattered aggregates were not present in experiments conducted with carboxy-terminated SERS-633, though strong Raman signal selectively remained in those layers with the antigen of interest (**Figure 4f**). Based on these results, it may be concluded that surface functionalization greatly affects the ability of colloidal SERS-active Au NPs to aggregate on the surfaces of cross-sectional art samples.

Additionally, we observed a tendency toward aggregation of both amino-terminated and carboxy-terminated SERS-633 over time. Since increased aggregation was observed within the storage lifetime of Au NP-conjugated secondary antibody (approximately 12 months), it is possible that this phenomenon results from electrostatic interactions of the protective PEG coating as well as degradation of SERS-tagged antibodies. A heightened tendency toward aggregation over time might also be related to delocalization of pi-electrons and steric effects associated with Au NP surface coating, which have been used to explain observed increases in lifetime of the DBDT reporter signal (greater than 3 months) when employed as an Au NP linker molecule [24].

Comment [EP13]: Referee: 1

Comment [EP14]: ... but lies outside the scope of the current study.

Comment [EP15]: Referee: 2

Comment [EP16]: Referee: 2: Commercial SERS-440 tags showed lower selectiveness for protein antigen in multilayer cross-sections, and a tendency toward non-specific aggregation on the sample surface. This made it necessary to create our own SERS-633 tags for use on art samples.

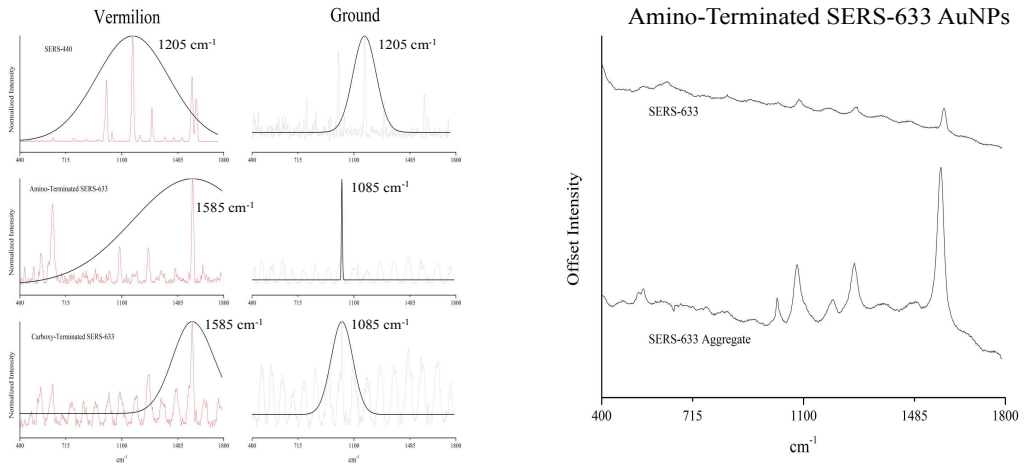

Figure 5a. Averaged immuno-SERS spectra from Replica Sample 2 demonstrate robust signal and heightened specificity of carboxy-terminated SERS-633 compared to commercial SERS-440 AuNPs. Commercial SERS-440 AuNPs (top) show reporter signal at 1205 cm^{-1} (single amplitudinal Gaussian fit, solid black line) in both vermilion/ovalbumin paint layer (red) and in ground/glue layer (light grey). Amino-terminated (middle) and carboxy-terminated SERS-633 AuNPs (bottom) show DBDT reporter signal at 1585 cm^{-1} only in the vermilion/ovalbumin paint layer. A sharp peak at 1085 cm^{-1} from the CO_3^{2-} stretching of the calcite ground is observed in both cases. SERS-440 spectra collected with a 20x objective and 785 nm laser excitation (10 s integration time, 10 mW). SERS-633 spectra collected with a 20x objective and 633 nm He Ne laser excitation (10 s integration time, 2.5 mW). All spectra are baseline corrected and normalized. **Figure 5b.** Immuno-SERS spectra from Replica Sample 2 show distinct intensity changes between excitation of amino-terminated SERS-633 aggregates and non-aggregated AuNPs on the sample surface. Spectra are single measurements and have not been corrected for baseline.

To explore the robustness of the immuno-SERS method and specificity of SERS-633 tags, as well as the tendency of the nanoparticles to aggregate, additional replica samples of inorganic pigments bound with whole egg were tested (**Figure 5**). Replica Sample 2 consisted of one pigment/binder combination of vermilion/whole egg-bound layer (~80 µm wide) prepared on gesso ground (~230 µm wide) in a traditional manner [34]. Commercial SERS-440 tags showed non-specific binding of secondary antibody-tagged Au NPs, as confirmed by the presence of characteristic reporter signal [21] in the ground/animal glue-bound layer of Replica Sample 2 (**Figure 5a**, top). Both amino-terminated and carboxy-terminated SERS-633 tags showed strong DBDT reporter signal only in the vermilion/whole egg-bound layer, indicated by Gaussian distributions centered at 1585 cm^{-1} (**Figure 5a**, middle, bottom). A strong, sharp calcite peak at 1085 cm^{-1} was found in ground layers assayed with amino-terminated and carboxy-terminated SERS-633 tags.

Visible aggregates were observed across the surface of Replica Sample 2 when probed for the presence of ovalbumin with commercial SERS-440 tags and amino-terminated SERS-633 tags, respectively (data not shown). In contrast, carboxy-terminated SERS-633 tag aggregates were not observed under visible light.

In general, the presence of heavy metal-containing pigments should not affect inherent aggregation properties of carboxy-terminated SERS-633 tags. Several colorimetric assays based on the aggregation of surface functionalized Au NPs have been developed for the detection of aqueous metal ions, including Pb^{2+} [35], Cu^{2+} [36], and Hg^{2+} [37] species. Liu et al. (2010) utilized the high log K_f of $Hg(SH)_n$ relative to $Au(SH)_n$ to abstract a quarternary ammonium-thiol bi-functionalized surface coating from Au NPs, which induced the aggregation of Au NPs [38]. Thus, there is evidence for the release of ammonium-thiol compounds from amino-terminated ligands on Au NPs. This may explain the higher tendency of our amino-terminated SERS-633 tags to aggregate. Based on our observations, however, surface topography and chemistry of different art sample preparations also contribute to undesired aggregation. We conclude that our non-commercial carboxy-terminated SERS-633 tags show high antigen specificity for the study of proteinaceous binding media in art samples, and are unaffected by heavy-metal presence in inorganic pigments [38-40]. Moreover, carboxy-terminated SERS-633 tags appear less sensitive toward surface topography or chemistry, and therefore do not display significant aggregation. A more comprehensive analysis of the effects of heavy metal-containing pigments on immuno-SERS systems is warranted, although this lies outside of the scope of the present study.

The formation of amino-terminated SERS-633 tag aggregates prompted us to confirm whether we could differentiate direct laser excitation of aggregates from disperse SERS-633 tags (**Figure 5b**). While both measurements showed significant, detectable peaks consistent with DBDT reporter

Comment [EP20]: Referee 2: (Figure 5) The Gaussian curves are automatically fit to spectra as described above (Experimental, Raman Data Analysis). Line widths of the Gaussian are merely related to the presence of multiple peaks in the spectrum: for example, multiple peaks arising from the Raman chemical signature spectrum of the commercial SERS-440 particles widen the Gaussian. However, due to issues of quantitative analysis of SERS data described above, width of the Gaussian in general cannot be associated with any physical quantity within our experimental system. The significant aspect is the presence or absence of a Gaussian centred about the most prevalent signal from the SERS reporter.

Comment [EP18]: Referee: 2: The article from Major and Zhu (JACS, 2003) describes coordination to Cu2+ cations by -COOH groups adsorbed to gold surfaces as a monolayer. We describe the differences between our SERS system and monolayer preparations above. Furthermore, our conclusions are supported by our results using Replica Sample 2 (vermilion, HgS) as a test case, which does not seem to encourage aggregation of carboxy-terminated SERS-633 or interfere with the selectivity of our SERS-633 particles for protein antigen (as no SERS-633 signal was detected in the ground layers, Fig 5a). Huang and Chang (*Chem Comm*, 2007, 1215-1217) have described the capture of Hg2+ cations by acid groups on Au NPs in aqueous solution, but because we report no tendency toward aggregation for our SERS-633 Au NPs when tested on vermilion samples, this possibility can be ruled out.

Comment [EP19]: Referee: 2

Comment [EP17]: Referee: 2: The heavy metals found in inorganic pigments have very low-solubility in aqueous systems, and it is therefore likely that they would not be at risk of interfering with the functionality of our SERS-633 particles (ie leading to aggregation, chemical interferences, etc.).

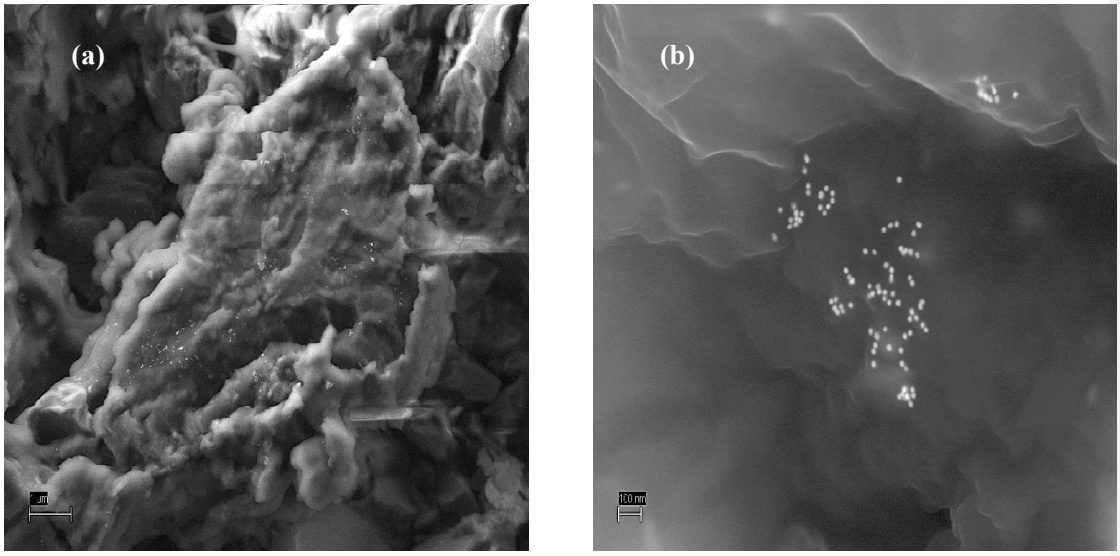

Figure 6. SEM images of carboxy-terminated SERS-633 bound to ovalbumin media *in situ* (Replica Sample 1, French ochre/ovalbumin layer) at (a) 9000x and (b) 49500x magnification demonstrate the specificity of SERS-633 for proteinacious binding media and preservation of discrete (~50 nm) dimer units.

pattern, major intensity differences between the two cases are noticeable. Though significant intensity differences can ensure a specific SERS signature is an indicator of protein presence in a sample rather than mere excitation of proximate Au NP aggregates, researchers should be cautious when interpreting immuno-SERS results conducted with probes prone to aggregation. Carboxy-terminated SERS-633 Au NP-antibody constructs aid in proper interpretation of immuno-SERS results as they overcome aggregation in the detection and localization of organic media in artworks.

Finally, we explored the ability of carboxy-terminated SERS-633 tags to remain as dimers when bound to ovalbumin-rich media *in situ* (**Figure 6**). Low magnification SEM imaging showed Au NPs to be evenly dispersed over the surfaces of organic globules in the french ochre/whole egg-bound layer of Replica Sample 1 (**Figure 6a**). Au NP clusters were localized in the organic regions, away from surrounding inorganic materials. With increasing magnification, SEM imaging revealed that Au NPs largely retained their original dimeric structures and spherical morphologies. While some monomeric impurities remained from the original SERS-tag preparations, these were proven not to influence the performance of the assay. Moreover, Au NP dimers measured approximately 50nm in total diameter when attached to binding media in a cross-section (**Figure 6b**). This agrees with our initial characterization of the as-made tag samples (see TEM micrographs in **Figure 2b**). Minimal clustering, preference for proteinaceous media, and preserved dimeric organization of carboxy-terminated SERS-633 tags throughout the immuno-SERS protocol support the hypothesis that localization of tags arises from specific antigen-antibody binding interactions. The carboxy-terminated SERS-633 tag serves as an accurate, indirect reporter of protein presence in art samples.

Conclusions

We have reported on the conjugation of polyclonal secondary antibodies to colloidal Au NP dimers functionalized with X'-PEG-SH (X' = -NH_2 or -COOH) to be used as SERS tags for the detection and localization of protein-based binding materials in artworks. The indirect immuno-SERS assay can be accomplished with relatively inexpensive materials and instrumentation found in most cultural heritage laboratories. Furthermore, our assay can provide information not readily available with present methods. These advantages offer great potential for field use, as well as application in laboratory settings. In relation to other immunological techniques, the immuno-SERS protocol allows for the micro-destructive investigation of intact samples, providing critical data on the spatial distribution of proteins within the stratigraphy of cross-sectional art samples.

Until now, the greatest obstacle to widespread application of the immuno-SERS method was the non-specific aggregation of Au NPs. Our investigation of SERS-active Au NPs shows that these carboxy-terminated surface coatings most effectively eliminate aggregation, without significant loss of reporter signal. Aggregation of Au NPs also shows a clear dependence on the chemical identity of protective PEG coating. Thus, we conclude that the maintenance of disperse Au NPs may be promoted by cumulate negative charges across the gold surface,

resulting from de-protonation of carboxyl functional groups in working buffer. Raman results show that the carboxy-terminated SERS-633 reporting system in the immuno-SERS method offers high antigenic specificity and resilience to pigment interference. Visible light and scanning electron microscopy reveal no tendency toward aggregation on the sample surface, and preservation of discrete Au NP dimers throughout the assay.

Future work will address possibilities for protein detection assays with other molecular probes, as well as novel SERS Au NPs of various shapes and protective surface coatings. We will also investigate proteinaceous media and antigen-antibody interactions in artworks as they change over time. Immuno-SERS techniques and other antibody-based methods promise to reveal new insights into artists' use of proteinaceous binding media, and implications for the sustained preservation of objects of cultural heritage.

Acknowledgements

The authors acknowledge Federico Carò (Department of Scientific Research, The Metropolitan Museum of Art, New York) for assistance with scanning electron microscopy, Julia Schultz (Stuttgart State Academy of Art and Design, Germany) for preparation of Replica Sample 1, and Brian Baade (Art Conservation Department, University of Delaware, Newark, Delaware) for preparation of Replica Sample 2. This work is supported by a grant from the National Science Foundation to the Metropolitan Museum of Art and Columbia University (NSF Award CHE 1041839).

Notes and references

[a] Department of Scientific Research, The Metropolitan Museum of Art, 1000 Fifth Avenue, New York, NY 10028, USA.
[b] Department of Materials Science and Engineering, Institute for Advanced Materials Devices and Nanotechnology, Rutgers University, 607 Taylor Road, Piscataway, NJ 08854, USA.

Corresponding Author: Julie Arslanoglu, julie.arslanoglu@metmuseum.org, Work: +1 (212) 396-5534, Fax: +1 (212) 396-5466

Electronic Supplementary Information (ESI) available: Replica Sample 1 immuno-SERS measurements under 20x and 50x objectives.

1 J. Arslanoglu, J. Schultz, J. Loike and K. Peterson, *J. Biosci.*, 2010, **35**, 3-10.
2 M. Gambino, F. Cappitelli, C. Catto, A. Carpen, P. Principi, L. Ghezzi, I. Bonaduce, E. Galano, P. Pucci, L. Birolo, F. Villa and F. Forlani, *J. Biosci.*, 2013, **38**, 397-408.
3 A. Rizzo, *Anal. Bioanal. Chem.*, 2008, **392**, 47-55.
4 K. Keune, F. Hoogland, J. J. Boon, D. Peggie and C. Higgit, *International Journal of Mass Spectrometry*, 2009, **284**, 22-34.
5 A. Atrei, F. Benetti, E. Gliozzo, G. Perra and N. Marchettini, *International Journal of Mass Spectrometry*, 2014, **369**, 9-15.
6 A. Heginbotham, V. Millay and M. Quick, *J. Am. Inst. Conserv.*, 2006, **45**, 89-105.
7 L. Cartechini, M. Vagnini, M. Palmieri, L. Pitzurra, T. Mello, J. Mazurek and G. Chiari, *Accounts of Chemical Research*, 2010, **43**, 867-876.
8 G. Sciutto, L. S. Dolci, M. Guardigli, M. Zangheri, S. Prati, R. Mazzeo and A. Roda, *Anal. Bioanal. Chem.*, 2013, **405**, 933-940.
9 A. Hakonen, P. O. Andersson, M. S. Schmidt, T. Rindzevicius and M. Käll, *Anal. Chim. Acta*, 2015, doi: 10.1016/j.aca.2015.04.010.
10 A. S. D. S. Indrasekara, S. Meyers, S. Shubeita, L. C. Feldman, T. Gustafsson and L. Fabris, *Nanoscale*, 2014, **6**, 8891-8899.
11 J. Chen, Y. Huang, S. Zhao, X. Lu and J. Tian, *Analyst*, 2012, **137**, 5885-5890.
12 P. Zijlstra, P. M. R. Paulo and M. Orrit, *Nat. Nano.*, 2012, **7**, 379-382.
13 P. L. Stiles, J. A. Dieringer, N. C. Shah and R. P. Van Duyne, *Annu. Rev. Anal. Chem.*, 2008, **1**, 601-626.
14 N. J. Halas, S. Lal, W.-S. Chang, S. Link and P. Nordlander, *Chem. Rev.*, 2011, **111**, 3913-3961.
15 A. Hakonen, M. Svedendahl, R. Ogier, Z.-J. Yang, K. Lodewijks, R. Verre, T. Shegai, P. O. Andersson and M. Käll, *Nanoscale*, 2015, **7**, 9405-9410.
16 A. S. D. S. Indrasekara, R. Thomas and L. Fabris, *Phys. Chem. Chem. Phys.*, 2015, doi: 10.1039/c4cp04517c.
17 L.-L. Tay, Q. Hu, M. Noestheden and J. P. Pezacki, *Proc. of SPIE*, 2007, *6450*.
18 Y. Kitahama, T. Itoh, P. Pienpinijtham, S. Ekgasit, X. X. Han and Y. Ozaki, *Functional Nanoparticles for Bioanalysis, Nanomedicine, and Bioelectronic Devices*, 2012, **2**, 181-234.
19 Y. Wang, L.-J. Tang and J.-H. Jiang, *Anal. Chem.*, 2013, **85**, 9213-9220.
20 M. H. Shin, W. Hong, Y. Sa, L. Chen, Y.-J. Jung, X. Wang, B. Zhao and Y. M. Jung, *Vibrational Spectroscopy*, 2014, **72**, 44-49.
21 J. Arslanoglu, S. Zaleski and J. Loike, *Anal. Bioanal. Chem.*, 2011, **399**, 2997-3010.
22 G. Sciutto, L. Litti, C. Lofrumento, S. Prati, M. Ricci, M. Gobbo, A. Roda, E. Castellucci, M. Meneghetti and R. Mazzeo, *Analyst*, 2013, **138**, 4532-4541.
23 P. L. Jones, *Studies in Conservation*, 1962, **7**, 10-16.
24 A. S. D. S. Indrasekara, B. J. Paladini, D. J. Naczynski, V. Starovoytov, P. V. Moghe and L. Fabris, *Adv. Healthcare Mater.*, 2013, 1-7.
25 OriginLab v.7 User Guide
26 M. Bradley, *Thermo Fisher Scientific*, 2007, Application Note: 50733.
27 K. S. Mayya, V. Patil and M. Sastry, *Langmuir*, 1997, **13**, 2575-2577.
28 A. Kumar, A. B. Mandale and M. Sastry, *Langmuir*, 2000, **16**, 6921-6926.
29 D. B. Pedersen and E. J. S. Duncan, *Defence R&D Canada*, 2005.
30 F. Ospitali, D. Bersani, G. Di Lionardo and P. P. Lottici, *J. Raman Spectrosc.*, 2008, **39**, 1066-1073.
31 M. De La Pierre, C. Carteret, L. Maschio, E. Andre, R. Orlando and R. Dovesi, *J. Chem. Phys.*, 2014, **140**, 1-12.

Comment [EP21]: Referee: 1

Formatted: Font: Times New Roman, 8 pt, Spanish (International Sort), Character scale: 105%

32 J. L. Perez-Rodriguez, M. D. Robador, M. A. Centeno, B. Siguenza and A. Duran, *Spectrochemica Acta Part A: Molecular and Biomolecular Spectroscopy*, 2014, **120**, 602-609.

33 R. Mukhopadhyay, *Chemistry World*, 2010, 44-47.

34 D. V. Thompson, Jr., *The Practice of Tempera Painting Materials and Methods*, Dover Publications, Inc., New York, 1962, 25-27.

35 J. Liu and Y. Lu, *J. Am. Chem. Soc.*, 2005, **127**, 12677-12683.

36 C.-H. Lu, Y.-W. Wang, S.-L. Ye, G.-N. Chen and H.-H. Yang, *NPG Asia Materials*, 2012, **4**, 1-7.

37 C.-C. Huang and H.-T. Chang, *Chem. Commun.*, 2007, 1215-1217.

38 D. Liu, W. Qu, W. Chen, W. Zhang, Z. Wang and X. Jiang, *Anal. Chem.*, 2010, **82**, 9606-9610.

39 J. Aguado, J. Arsuaga, A. Arencibia, M. Lindo and V. Gascon, *Journal of Hazardous Materials*, 2009, **163**, 213-221.

40 Y. Kim, R. C. Johnson and J. T. Hupp, *Nano Lett.*, 2001, **1**, 165-167.

Formatted: Font: Times New Roman, 8 pt, Spanish (International Sort), Character scale: 105%

Formatted: Spanish (International Sort)